

Péter Árkai · Shah Wali Faryad · Olivier Vidal
Kadosa Balogh

Very low-grade metamorphism of sedimentary rocks of the Meliata unit, Western Carpathians, Slovakia: implications of phyllosilicate characteristics

Received: 21 November 2001 / Accepted: 17 October 2002 / Published online: 30 January 2003
© Springer-Verlag 2003

Abstract The Meliata unit represents a *mélange*-like accretionary wedge, containing blueschist facies tectonic blocks and slices in a Triassic and Jurassic sedimentary matrix. The blueschist facies rocks are tectonic remnants of the subducted parts of the Meliata-Hallstatt branch of the Tethys. The phyllosilicate assemblages in very low-grade metapelites represent metastable disequilibrium stages which the assemblages have reached during reaction progress. Therefore, temperature and pressure values of low-T metamorphism of the sedimentary series and the late stages of decompressional cooling of blueschist facies rocks, obtained by phyllosilicate “crystallinity”, chlorite thermometric and white K-mica geobarometric methods, can be regarded as semiquantitative estimates. However, results of chlorite–white mica thermobarometry suggest that local equilibrium was approached at a microscopic scale. For deciphering the age relations of prograde and retrograde events, K–Ar isotope geochronological methods were applied. The sedimentary series and related basalts of the Meliata unit experienced high-T anchizonal prograde regional metamorphism, the temperature and pressure of which can vary between ca.

280 and 350 °C and ca. 2.5 and 5 kbar. White K-mica *b* geobarometry suggests possible minimal pressures of ca. 1.5 to 3 kbar. The mylonitic retrogression of blueschist facies phyllites is characterised by 340 °C and 4 kbar (minimal P). The low-T prograde metamorphism was synchronous with the retrograde metamorphism of the blueschists. The ages of these two events may be between ca. 150 and 120 Ma, culminating most probably at around 140–145 Ma. Thus, the Upper Jurassic (lowermost Cretaceous) very low-grade metamorphism of the Meliata unit is younger than the subduction-related, 160–155 Ma blueschist facies event, and definitely older than the Cretaceous (100–90 Ma) metamorphism of the footwall Gemer Palaeozoic.

Keywords Accretionary metamorphism · Very low-grade metamorphism · Illite–white mica · Chlorite · Western Carpathians

Introduction

Accretionary wedges often contain high-pressure metamorphic blocks and slices – ranging from several decimetres to several kilometres in size – tectonically emplaced in unmetamorphosed or only slightly metamorphosed, usually clastic sedimentary matrix. Metamorphic features of the various constituents of these *mélanges* may elucidate the physical conditions (pressure–temperature paths) of subduction, collision and subsequent uplift (decompressional cooling) of the upper oceanic crust and related rocks of the accretionary prism. Contrasting the ophiolitic metabasites, metaclastic rocks are commonly devoid of indicative metamorphic mineral assemblages. Therefore, characterisation of phyllosilicate reaction progress complemented with rock microstructural features is practically the only tool for providing information on conditions of eventual incipient metamorphism.

The aim of this paper is to present new data on the sedimentary (mostly fine-clastic) rocks from a prominent

P. Árkai (✉)
Laboratory for Geochemical Research,
Hungarian Academy of Sciences,
Budaörsi út 45, 1112 Budapest, Hungary
e-mail: arkai@geochem.hu
Tel.: +36-1-3193137, Fax: +36-1-3193137

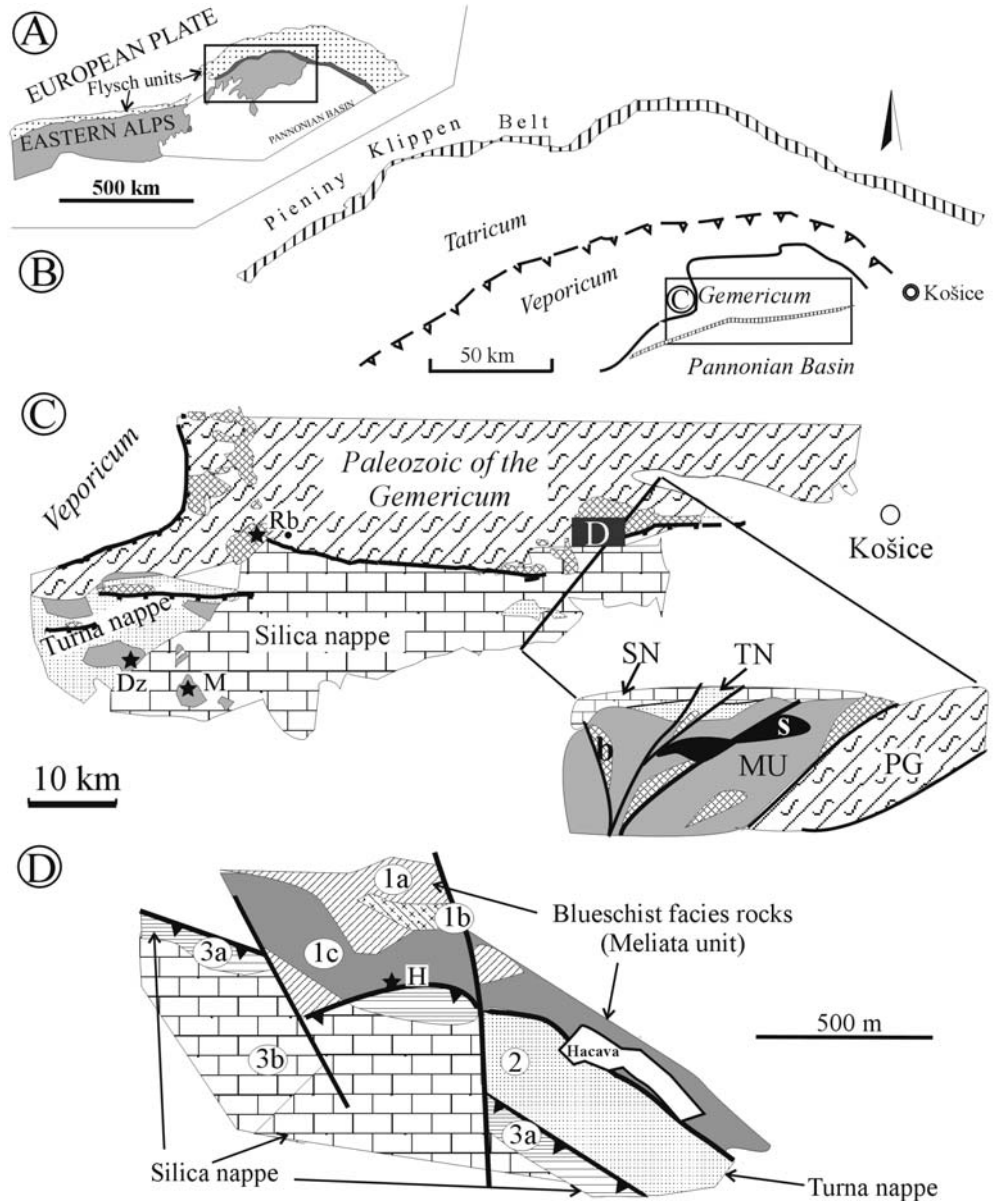
S. W. Faryad
Department of Geology and Mineralogy,
Technical University Kosice,
Letna 9, 04200 Kosice, Slovakia

O. Vidal
Maison des Geosciences, LGCA, Université Joseph Fourier,
1381 Rue de la Piscine, B.P. 53, 38041 Grenoble cedex, France

K. Balogh
Institute of Nuclear Research, Hungarian Academy of Sciences,
Bem tér 18/c, 4001 Debrecen, Hungary

S. W. Faryad
Institute of Petrology and Structural Geology, Charles University,
Albertov 6, 128 43 Prague 2, Czech Republic

Fig. 1 A Sketch of the Alpine–Carpathian–Pannonian system. B Position of the Meliata unit in the frame of the Western Carpathians. C Schematic geological map of the Meliata unit and its surroundings with an idealised cross section showing (from top to bottom): the Silica nappe (SN), Turna nappe (TN), Meliata unit (MU) with tectonic blocks of serpentinites (*s*) and blueschists facies rocks (*b*), Palaeozoic of the Gemicum (PG). D Detailed geological locality at the Hačava locality: 1 blueschist facies rocks (1a phyllites, 1b metabasalts, 1c marbles), 2 Turna nappe phyllites, 3 Silica nappe (3a limestones, 3b dark limestones with hematite). Stars in C and D indicate sample location: M Meliata, Dz Držkovce, Rb Rožňavské Bystre, and H Hačava



and strongly debated complex called the Meliata unit of the inner Western Carpathians, Slovakia (Fig. 1A, B; for general descriptions see Mock 1978; Árkai and Kovács 1986; Kozur and Mock 1996; Mello et al. 1996). The Meliata unit is considered as a southward-dipping accretionary complex between the footwall Palaeozoic of the Gemicum and the hanging wall, mostly Mesozoic Silica and Turna nappes (Fig. 1C, D). As the Meliata unit is built up by very low-grade metamorphic sedimentary rocks containing tectonic blocks of blueschists, it is plausible to suppose that at least some of these sedimentary rocks had a common history with the blueschists during the late stages of their exhumation.

The origin and metamorphic history of Meliata blueschists and related, high-P metasedimentary rocks, which either form isolated slices having been overthrust onto the Palaeozoic of the Gemicum or tectonic blocks within the incipient metamorphic sedimentary sequences, are

fairly well constrained by the recent works of Faryad (1995, 1997), Ivan and Kronome (1996), Mazzolli and Vozárová (1998) and Horváth (2000). By contrast, only sporadic data are available on the metamorphism of the sedimentary matrix of the Meliata mélangé (Árkai and Kovács 1986). Therefore, in order to provide comprehensive metamorphic petrogenetic data on the sedimentary rocks of the Meliata unit, systematic phyllosilicate (illite and chlorite) “crystallinity” studies, complemented with chlorite thermometry, white K-mica geobarometry, chlorite–white mica thermobarometry, and K–Ar isotopic dating of white K-micas, were carried out.

Geological setting, materials

Recently, the geology of the Meliata unit has been widely discussed with respect to its geotectonic position and

the petrological characteristics of its sedimentary rocks, blueschists and serpentinites (Hovorka et al. 1985; Mello 1993; Faryad 1995; Ivan and Kronome 1996; Kozur and Mock 1996; Mello et al. 1996). In the geological map of Mello et al. (1996), five tectonic units are distinguished in the South Gemic area. These are (from top to the bottom):

1. the Silica nappe with Triassic and Jurassic limestones, dolomites, with rare marls, shales and Permian evaporite;
2. the Turna nappe consisting of Triassic limestones, dolomites, marls and slates, locally of evaporites, and Permian, upper Carboniferous sandstones and conglomerates;
3. the Meliata unit containing Triassic and Jurassic slates, sandstones, marls, metabasalts, serpentinites and radiolarites;
4. the Borka nappe, represented only by blueschist facies rocks;
5. the Early Palaeozoic greenschist facies rocks of the Gemicum with Late Palaeozoic cover sequences.

The Meliata rocks are not widely exposed on the surface, although their abundant occurrence beneath the Silica and Turna nappes was confirmed by several boreholes. In addition to basalts and serpentinites, the Meliata unit contains also tectonic blocks of the Turna nappe (limestones and evaporites) and of the Silica nappe (sandstones and evaporites; Mello et al. 1996). Tectonic blocks of blueschists were found in the sedimentary series of the Meliata unit both in Slovak and Hungarian territories (Faryad and Dianiska 1999; Horváth 2000). Thus, separation of blueschists from the Meliata unit and their definition as a nappe was argued by Faryad (1998), who preferred the earlier interpretation of the Meliata unit as a mélangé complex (see Leško and Varga 1980; Mahel' 1986). Because of the contrasting rheology, some slices of blueschist facies rocks were probably separated from the Meliata complex and were overthrust onto the Early Palaeozoic of the Gemicum.

Samples used in this study derive from the Meliata unit and they were collected from four localities (Fig. 1C, D), namely from Meliata, Držkovce, Hačava and Rožňavské Bystre.

1. The rocks exposed in the Meliata type locality belong to the most common Liassic-Malmian sequence (dark grey slates, sandstones, spotty marls, dark limestones) and to an Aegean-Pelsonian sequence (light crystalline limestone). In addition to radiolarites and cherts, small amounts of basaltic rocks are also present. The investigated samples belong to the Liassic-Malmian sequence (M1–M13) and to metabasites (Fg9/01 and Fg10/01), which are exposed ca 1.5 km westwards from the village of Meliata.
2. The Meliata rocks (pelitic, pelitic-silty and carbonatic slates) are found also beneath the Turna nappe westwards from Držkovce village (Dz1–Dz13).
3. Pelitic-marly slates and limestone from Hačava (H2–H13) come from a tectonic zone between the

Meliata unit and the overlying Silica nappe. It is not clear whether these rocks belong to the Meliata unit or to the Turna nappe. According to the relevant geological map of Mello et al. (1996), rocks of the Turna nappe are exposed on the south-western side of the valley in which the village Hačava is located, and occur along the boundary between the Silica nappe and Meliata unit (Fig. 1D). The rocks of the Turna nappe are represented by recrystallised limestones, volcanoclastic rocks, slates and sandstones. The hanging-wall Silica nappe rocks consist of white limestones at the top and dark, hematite-bearing limestones at the bottom. The footwall Meliata rocks consist of blueschist facies marble and phyllite.

4. From a locality near to the village Rožňavské Bystre, mylonitised blueschists (Rb1–Rb8) were selected for this study. The Meliata rocks mapped here as Liassic-Malmian sequences by Mello et al. (1996) are actually mylonitised blueschist facies phyllites with relic chloritoid and pseudomorphs of albite and chlorite after glaucophane.

Methods

In order to determine the rock types, their microstructural (textural) features and modal compositions, detailed petrographic microscopic observations were made. Sample preparation techniques and the X-ray powder diffractometric (XRD) instrument and methods applied were the same as described by Árkai et al. (2000). For calibrating the XRD full width at half maximum (FWHM) data measured on the first- (and second-) order basal reflections of the phyllosilicates, a standard rock slab series (nos. 32, 34 and 35) kindly provided by B. Kübler was used. Thus, the illite "crystallinity" (KI=Kübler index) boundaries of the anchizone correspond to 0.25 and 0.42 $\Delta^\circ 2\theta$ in the present paper. On the basis of this calibration, using also the linear regression equations between KI and chlorite "crystallinity" (ChC) indices determined by Árkai et al. (1995b), the actual ranges of the anchizone are 0.26–0.38 $\Delta^\circ 2\theta$ for ChC(001), and 0.24–0.30 $\Delta^\circ 2\theta$ for ChC(002). All of these boundary values refer to air-dry (AD) mounts. For differentiation between K-, Na- and Ca-rich white micas, the XRD (00,10) basal reflections around 2 Å were used (see Frey and Niggli 1972).

White K-mica geobarometry elaborated for lower greenschist facies pelitic rocks by Sassi (1972) and extended to the high-T part of the anchizone by Padan et al. (1982) was applied for semi-quantitative estimation of metamorphic pressure conditions. For geobarometric estimations, the constraints given by Guidotti and Sassi (1976, 1986, 1998) were also taken into consideration. The $b=6 \times (d_{331,060})$ value was measured on disorientated whole rock and acid-insoluble residue, as well as on <2 μm grain-size fraction powder mounts as described by Árkai et al. (1991).

Mineral chemical analyses were obtained using a JEOL 6310-type scanning electron microprobe equipped with wavelength- and energy-dispersive spectrometers at the Institute for Mineralogy, Crystallography and Petrology, University of Graz, Austria. Operating conditions were 15 kV and 10 or 15 nA, with counting time of 20 s. Pyrope (Mg, Al), adular (K), rutile (Ti), tephroite (Mn), jadeite (Na, Si) and andradite (Fe, Ca) were used as standards. A defocused beam was applied to the white mica and chlorite analyses.

Metamorphic temperatures were estimated by the chlorite–Al^{IV} geothermometer of Cathelineau and Nieva (1985) and its modified versions (for details, see the Results). Metamorphic P–T conditions were also calculated using the program TWQ (version 1.02; Berman 1991) with the Jun92.rgb updated database and the thermodynamic data and corresponding solid solution models from Vidal et al. (2001) for chlorites, and Parra et al. (unpublished data) for K-white micas. The P–T conditions for the equilibrium paragonite–K-white

mica–albite–chlorite–quartz–H₂O were calculated using a multi-equilibrium approach, as explained in Vidal and Parra (2000).

For K–Ar isotopic dating of the white K-mica-rich, <2 µm grain-size fraction samples, the potassium was determined by flame photometry using a Li internal standard and Na buffer. Interlaboratory standards nos. Asia 1/65, HD-B1, LP-6 and GL-0 as well as atmospheric Ar were used for controlling and calibrating isotopic analyses. Details of the methods and instruments applied in the Institute of Nuclear Research, Hungarian Academy of Sciences, Debrecen, and results of calibration are given elsewhere (Árkai et al. 1995a and Odin et al. 1982 respectively). K–Ar ages were calculated using the constants proposed by Steiger and Jäger (1977).

Results

Rock types, modal and bulk-rock major-element compositions

From the *Meliata* type locality pelitic, silty, marly-pelitic and pelitic-cherty slates and massive metabasalts were studied. Slates display mostly an irregular fracture cleavage arranged in two, crosscutting plane sets. Where sedimentary layering occurs, the first cleavage set is parallel to the bedding, whereas the second (crosscutting) one displays typical, S-like arrangements formed due to intense bedding-parallel shearing. Rarely, the cleavage surfaces are mildly crenulated. They never show silky sheen. Slates consist of quartz, white K-mica (illite–muscovite) and chlorite ± variable amounts of calcite, small amounts of albite and traces of rutile. In their <2 µm grain-size fractions, illite–muscovite predominates, chlorite and quartz are significant, and albite, calcite and rutile appear only in subordinate and trace quantities, often lacking in certain samples. The massive, dark grey, aphanitic metabasalt samples are built up by quartz, albite, chlorite, carbonate minerals (calcite and ankerite) and various accessories.

From the *Držkovce* locality pelitic, pelitic-silty and carbonatic, locally banded slates (with several mm-thick sedimentary layers) were collected. Their mesostructural features resemble those of the *Meliata* slates. Both their whole-rock and <2 µm fraction samples are built up by white micas, quartz, chlorite, albite ± subordinate amounts of carbonate minerals (calcite and dolomite), pyrite and rutile. Sporadic presence of kaolinite is attributed to surficial weathering. As shown by Fig. 2, mixed K–Na-mica in traces or in subordinate quantities also occur, in addition to the predominant dioctahedral white K-mica (illite–muscovite).

From the *Hačava* locality pelitic-marly slates with fracture cleavage sets, lineation (“pencil” cleavage), as well as schistose, lineated limestone with white, mm-scale calcitic fissure fillings were investigated. The rocks contain white micas, chlorite, quartz, albite, calcite and, sporadically, dolomite, pyrite, hematite and rutile. In their <2 µm fractions, dioctahedral K-mica (illite–muscovite) predominates. In addition, discrete paragonitic mica as well as mixed K–Na-mica are also found in subordinate quantities (Fig. 2). Small amounts of smectite together with goethite indicate weak weathering.

Mylonite samples from the *Rožňavské Bystre* locality occur adjacent to rocks of blueschist facies assemblages

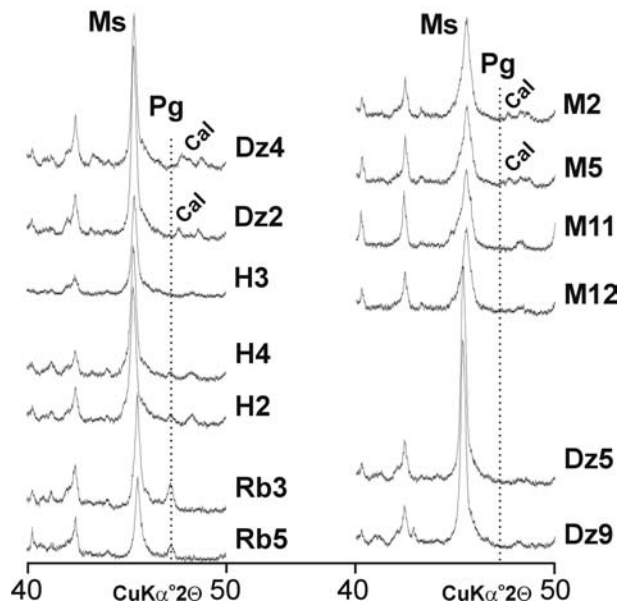


Fig. 2 Discrimination of white micas on the basis of their (00,10) basal reflections (after Frey and Niggli 1972): *Ms* white K-mica, *Pg* paragonite, *Cal* calcite. The peaks or shoulders between the *Ms* and *Pg* peaks refer to “mixed” K–Na-mica (for the interpretation of “mixed” micas, see Livi et al. 1997). Sample groups: *M* *Meliata*, *Dz* *Držkovce*, *H* *Hačava*, *Rb* *Rožňavské Bystre* (<2 µm fraction, air-dry, highly oriented samples)

with glaucophane, phengite and chloritoid (Faryad 1995). The mylonite displays irregular, wavy crenulation cleavage often with silky sheen, and fracture cleavage. In general, they are of slaty appearance, disregarding the metasandstone-like sample no. Rb7. These rocks consist of quartz and white micas. Chlorite, dolomite and relic chloritoid are sporadic and subordinate. Chlorite pseudomorphs after glaucophane can be also observed in some thin-sections. White micas are represented by dominant dioctahedral K-mica (phengitic muscovite) and considerable amounts of discrete paragonite, whereas the amounts of mixed Na–K-mica are subordinate (Fig. 2). In contrast to the rather simple, prograde microstructures of the slates from the localities *Meliata*, *Držkovce* and *Hačava*, the *Rožňavské Bystre* samples show clear evidence of polymetamorphism: white mica, quartz and, rarely, chloritoid porphyroclasts representing an earlier blueschist facies event are embedded in a fine-grained, foliated matrix consisting mainly of white micas and quartz. Goethite, kaolinite (and, in one sample, traces of smectite) indicate oxidative weathering.

XRD data of phyllosilicates

Figure 3 shows the histogram of the illite “crystallinity” (KI) data. The boundaries of the diagenetic, anchi- and epizones (sensu Kübler 1967, 1990) are also indicated in this figure (see also the Methods). The KI data correspond to the anchi-, and subordinately to the epizone, the maximum of the distribution being in the high-temperature part of the anchizone, very near to the boundary be-

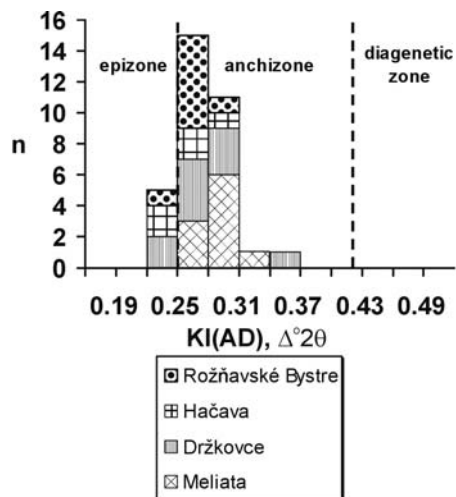


Fig. 3 Histogram of the illite “crystallinity” (KI) values measured on <2 μm fraction, air-dry samples

Fig. 4 Histograms of the chlorite “crystallinity” values measured on the 14- and 7-Å basal reflections, indicated as ChC(001) and ChC(002). Other conditions are as in Fig. 3

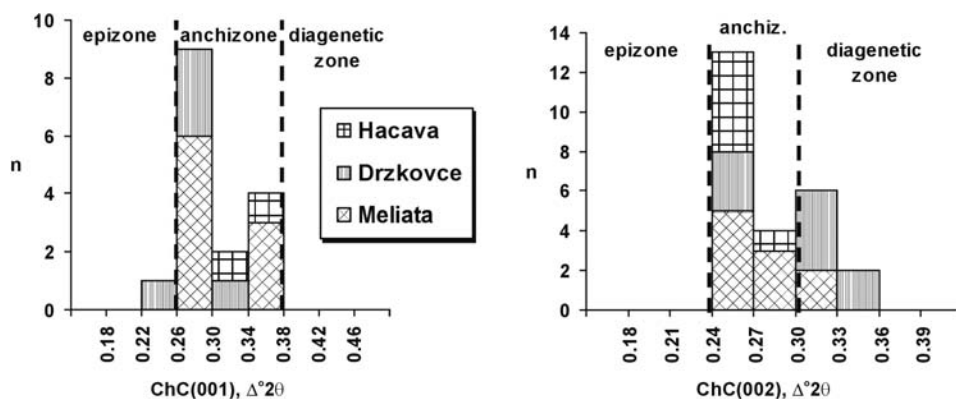


Table 1 Statistical parameters of illite Kübler-index (KI) and chlorite “crystallinity” values (ChC) expressed in $\Delta^\circ 2\theta$ (n number of samples, SD standard deviation)

	Meliata (M)	Držkovce (Dz) ^a	Hačava (H) ^b	Rožňavské Bystre (Rb) ^c
KI				
Mean	0.291	0.278	0.262	0.273
SD	0.026	0.029	0.015	0.016
n	10	10	5	8
Min.	0.252	0.244	0.246	0.243
Max.	0.338	0.341	0.281	0.302
ChC(001)				
Mean	0.308	0.356	0.278	0.331
SD	0.028	–	0.034	–
n	9	1	5	1
Min.	0.278	–	0.231	–
Max.	0.352	–	0.328	–
ChC(002)				
Mean	0.283	0.299	0.257	0.287
SD	0.019	0.032	0.007	–
n	10	9	5	1
Min.	0.265	0.253	0.249	–
Max.	0.323	0.340	0.265	–

^a KI values and their statistical parameters may be influenced by insignificant to minor amounts of paragonite

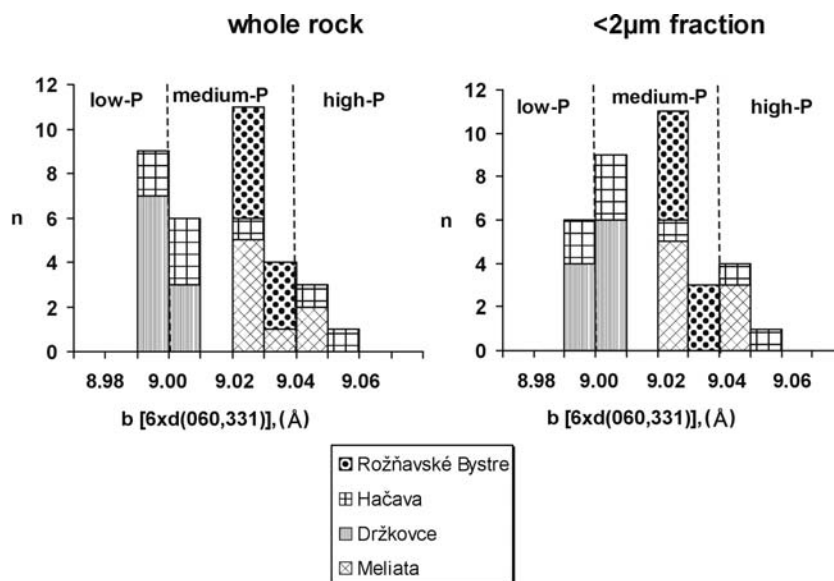
^b KI values and their statistical parameters may be influenced by minor amounts of paragonite

tween the anchi- and epizones. Considering the prograde series of the Meliata unit, a slight increase in grade (i.e. a slight decrease in KI averages) can be observed from the Meliata locality through Držkovce to Hačava (Table 1), although the amounts of mixed K-Na-micas and discrete paragonite increase in the same direction. This suggests that Na-bearing micas, being present in subordinate quantities as compared to white K-mica, may not have a significant effect on the FWHM values of the 10-Å basal reflections. The Rožňavské Bystre samples, containing the highest amounts of paragonite of the four sample groups, are characterised by a KI average which is very similar to the mean KI value of the Držkovce samples.

Similar conclusions can be drawn from the frequency distributions of the chlorite “crystallinity” data (Fig. 4), although the ranges here are narrower than that of the illite “crystallinity” scale and, consequently, the scatter in the values is relatively large. Thus, chlorite “crystallinity” averages (Table 1) follow only partially the above-

^c KI values and their statistical parameters may be influenced by subordinate amounts of paragonite

Fig. 5 Histograms of the white K-mica b values measured on unorientated powder mounts of bulk rock samples and on their $<2\ \mu\text{m}$ grain-size fractions. Pressure ranges are after Sassi (1972) and Guidotti and Sassi (1986)



mentioned trend, presumably because of the greater errors caused by the small XRD intensities, and partly because of the variation in chlorite composition.

From a thermodynamic point of view, the studied phyllosilicates and their “crystallinity” indices, as empirical parameters, document a certain stage in phyllosilicate reaction progress, which the investigated rock reached through a series of reactions producing phases which represent metastable disequilibria (for recent reviews, see Merriman and Peacor 1999, and Árkai 2002). Therefore, “crystallinity” indices and other phyllosilicate parameters of anchizonal rocks are theoretically inadequate for precise geothermometric and geobarometric calculations, because reaction progress is also controlled by kinetic factors.

In general, the approximate boundary between the anchi- and epizonal is placed between ca. 300 and 350 °C, as deduced from combinations of large datasets of KI, vitrinite reflectance, and fluid-inclusion with metabasite mineral facies data from various geotectonic regimes (e.g. Kisch 1983, 1987; Frey 1987; Merriman and Frey 1999). Consequently, T estimates for the investigated samples may be bracketed between ca. 270 and 350 °C.

Contrary to the uniform temperature conditions of metamorphism indicated by the phyllosilicate “crystallinity” data, the $b=6 \times d_{(060,331)}$ values of white K-mica are widely scattered (Fig. 5). The various localities are characterised by strongly differing b distributions, suggesting varying pressure conditions for the different sample groups. Distributions of b values measured on whole-rock samples and the $<2\ \mu\text{m}$ fractions are rather similar within each group, indicating pervasive homogenisation (crystallisation and recrystallisation) of white K-mica during metamorphism.

Disregarding the Meliata samples (in which no Na-containing micas could be detected by XRD), a considerable part of the samples from the other groups contains paragonite and/or mixed K-Na-mica. Consequently, con-

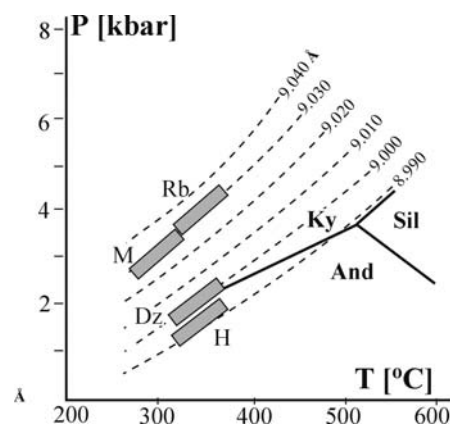


Fig. 6 P–T diagram with isopleths of white K-mica b values (after Guidotti and Sassi 1986). *M* Meliata, *H* Hačava, *Dz* Držkovce, *Rb* Rožňavské Bystre. P–T conditions are semi-quantitative estimates. Temperatures were derived from the phyllosilicate “crystallinity” averages and from the chlorite–Al^{IV} thermometer of Cathelineau and Nieva (1985; see also Table 5). The derived pressures are approximate minimum pressures in the case of the Hačava, Držkovce and Rožňavské Bystre sample groups

sidering also the constraints of Guidotti and Sassi (1976) on the effects of modal composition and bulk rock chemistry on white K-mica b values, systematically lower b values can be expected for these samples, and pressure estimates should be used only as approximate minimal P values. Table 2 displays the statistical parameters of white K-mica b values determined for each sample group. Based on the findings of Padan et al. (1982), Fig. 6 shows the linear extrapolation of isolines of b values given by Guidotti and Sassi (1986) for the P–T field of greenschist facies towards the anchizone (sub-greenschist facies). Accepting the temperature estimates of ~300 °C for the Meliata and ~340–350 °C for the other groups deduced from the illite Kübler-index data, the following approximate pressures can be estimated:

Table 2 Statistical parameters of white K-mica $b=6 \times d_{331.060}$ values expressed in Ångström (n number of samples, SD standard deviation)

Sample group	Statistical parameter	Whole rock			<2 µm fraction	
		All samples	Selected samples ^a (main group)	Selected samples ^a (subord.)	All samples	Selected samples ^a (main group)
Meliata (M)	Mean	9.031	9.029 ^a		9.032	9.027 ^a
	SD	0.007	0.007 ^a		0.01	0.007 ^a
	n	8	6 ^a		8	6 ^a
	Min.	9.023	9.023 ^a		9.022	9.022 ^a
	Max.	9.043	9.043 ^a		9.046	9.041 ^a
Držkovce (Dz)	Mean	9.000	9.002 ^a		9.002	9.003 ^a
	SD	0.002	–		0.003	–
	n	10	2 ^a		10	2 ^a
	Min.	8.998	9.002 ^a		8.997	8.997 ^a
	Max.	9.002	9.002 ^a		9.007	9.007 ^a
Hačava (H)	Mean	9.016	9.001	9.042	8.994	
	SD	0.023	0.005	0.005	0.007	
	n	8	5	3	4	
	Min.	8.999	8.994	9.029	8.985	
	Max.	9.058	9.008	9.058	9.003	
Rožňavské Bystre (Rb)	Mean	9.030			9.027	
	SD	0.003			0.004	
	n	8			8	
	Min.	9.028			9.022	
	Max.	9.035			9.032	

^a Data of selected samples with modal compositions which are strictly adequate for pressure estimation. Sample groups which may contain minor amounts of paragonite are indicated *italic*

Meliata: ~3 kbar; Držkovce: ~2 kbar (minimal P); Hačava: ~1.5 kbar (minimal P) with uncertain traces of an earlier, ~3–4 kbar event (minimal P); and Rožňavské Bystre: ~4 kbar (minimal P), with evidence of an earlier, higher-P event. However, it should be emphasised that the P–T brackets must be regarded as semiquantitative estimates at best, because of the disequilibrium, metastable nature of the systems and because of the shortcomings of the “bulk” methods used and discussed above in detail. Whereas the temperature estimates of prograde metamorphism of the metasedimentary formations (Meliata, Držkovce and Hačava) and the temperature estimates of retrogression of blueschist facies metapelites (Rožňavské Bystre mylonites) vary within a relatively narrow range, the estimates of possible minimal pressures show a much larger scatter, from ~1.5 to ~3 kbar for the prograde incipient metamorphic series, and indicating ~4 kbar for the retrogression of Rožňavské Bystre samples.

Phyllosilicate chemistry

Because of the small grain size of metamorphic phyllosilicates, special attention was paid to differentiation between inherited (detrital) and newly formed white K-micas and chlorite. Figure 7 shows some characteristic textural features. In certain cases (e.g. in the locality Meliata), detrital micas altered to white K-mica/chlorite stacks, and chloritic aggregates formed presumably after mafic silicates (Fig. 7a) could be easily distinguished

from fine-grained, matrix-forming white mica and chlorite flakes arranged mostly parallel to the metamorphic schistosity (Fig. 7b). In other samples, however, especially where the metamorphic (re)crystallisation was intense, a continuous transition could be observed between the finer and larger phyllosilicate flakes, all having been aligned into the plane of foliation (Fig. 7c, d). In Fig. 7d, metamorphic paragonite is intergrown and locally rimmed by phengitic white K-mica.

The chemical compositions of white K-mica and chlorite, as measured by EMP, are given in Tables 3 and 4 (the complete dataset of mineral chemical analyses, together with the X-ray diffractometric KI, ChC and b values can be obtained either in electronic or in printed forms upon request from the first author in the next three years).

The chemical criteria given by Vidal and Parra (2000) were used for selecting the EMP analyses without considerable contamination and/or loss of alkalis, thus being acceptable for further petrogenetic considerations. The plots of these selected analyses show significant celadonitic isomorphous substitution in muscovite. The deficiencies in K and Na indicate moderate proportions of the pyrophyllite end member (Fig. 8). Figure 9a–c demonstrates that the Tschermak'-type phengitic (or celadonitic) ${}^{\text{IV}}\text{Al}_{-1}{}^{\text{VI}}\text{Al}_{-1} \rightleftharpoons \text{Si}(\text{Fe}^{2+}, \text{Mg})$ substitution predominates in the newly formed (metamorphic) white K-micas. Ferric iron in white K-mica does not seem to be important because there are only minor deviations from the muscovite–celadonite mixing line (Fig. 9c). There is no significant correlation between the Fe and Mg contents either

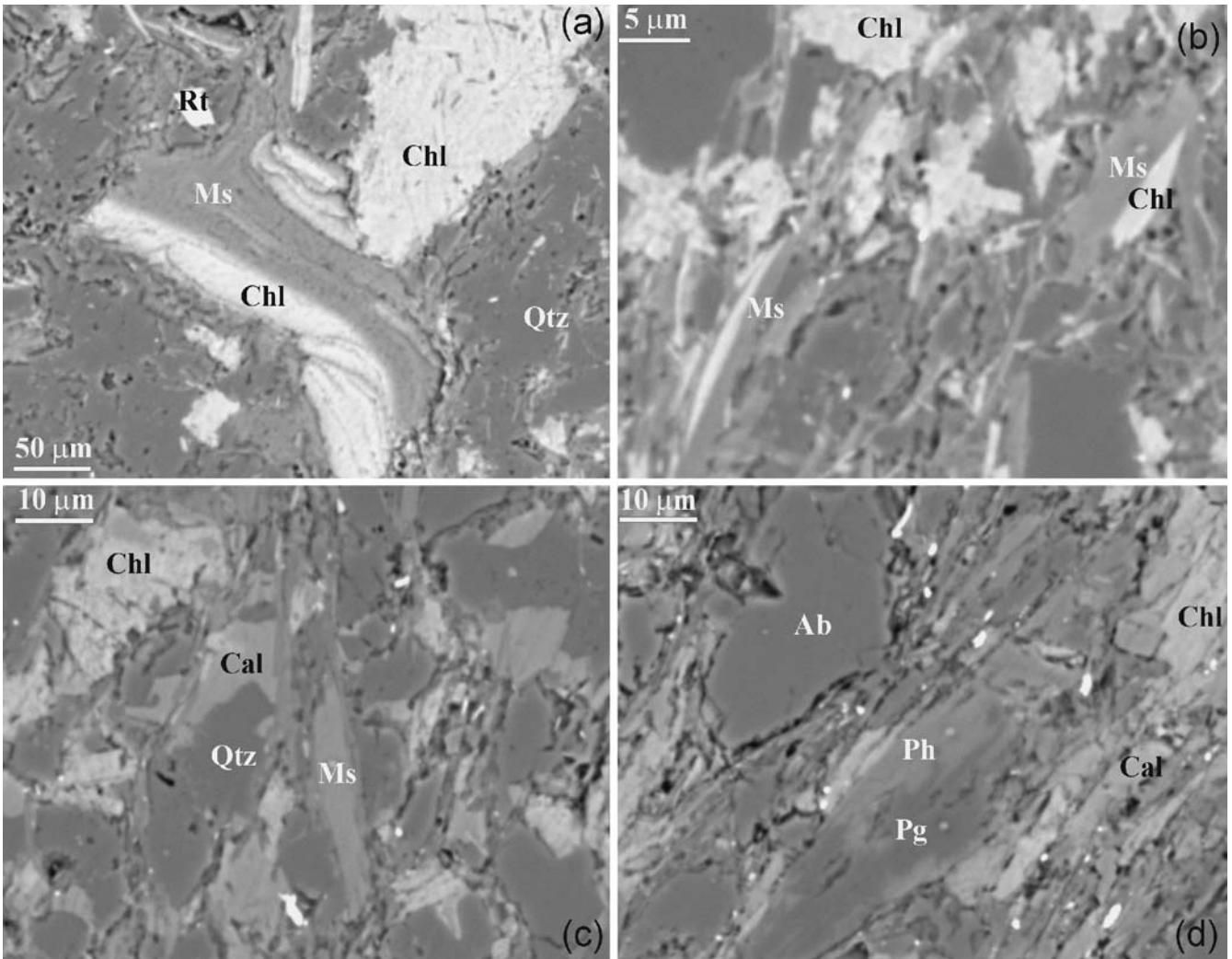
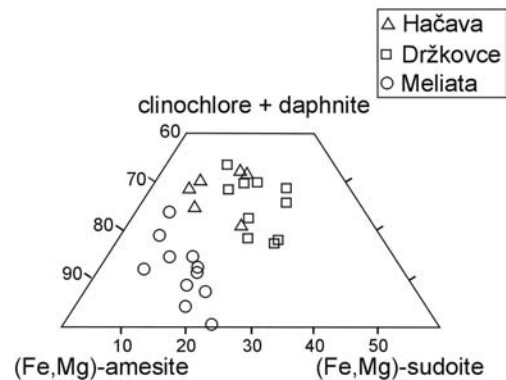
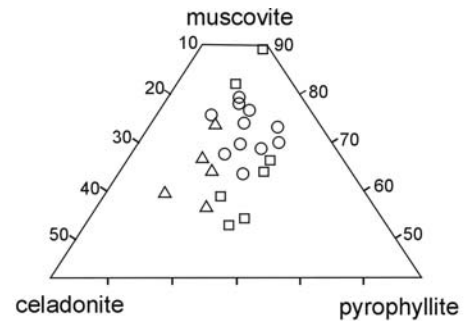


Fig. 7a–d Backscattered electron (BSE) images of textural relations of phyllosilicates in fine-grained metaclastic rocks. **a** Chlorite/white mica stacks after detrital mica and chloritic aggregates in sample Meliata M3. **b** Fine-grained, newly formed (metamorphic) white K-mica and chlorite in the matrix of metapelite (Meliata, sample M4). **c** Phyllosilicates with varying grain size in slate (Držkovce, sample Dz7). **d** Metamorphic paragonite closely associated and rimmed by phengitic white K-mica, all arranged in the plane of foliation. Locality Hačava, sample H2. Abbreviations of mineral names: *Ms* muscovite (white K-mica), *Ph* phengite, *Chl* chlorite, *Qtz* quartz, *Cal* calcite, *Ab* albite, *Rt* rutile



(Fig. 9d). On the basis of model calculations supposing various mixtures, the dotted arrows in Fig. 9a–c indicate those trends which white K-mica analyses contaminated by quartz or chlorite should follow. These trends differ significantly from those found in the present dataset. This fact, together with the chemical criteria of Vidal and Parra (2000), demonstrates that “contaminations” during EMP analyses caused by small grain size are negligible.

Fig. 8 Muscovite–celadonite–pyrophyllite and amesite–(clinochlore+daphnite)–sudoite ternary plots of selected white K-mica and chlorite analyses, using the criteria of Vidal and Parra (2000)

Table 3 Chemical compositions of white K-mica determined by EMP (weight% and cation numbers)

Sample	M1		M2		M3		M4		M3		Dz3		Dz5		Dz7		H2		H3		Rb3		Rb7						
	Met.	Detr.	Met.	Detr.	Met.	Detr.	Met.	Detr.	Met.	Detr.	Met.	Detr.	Met.	Detr.	Met.	Detr.	Met.	Detr.	Met.	Detr.	Met.	Detr.	Met.	Detr.	Met.	Detr.			
<i>n</i>	2	3	1	2	2	2	2	2	7	7	7	7	7	7	6	6	6	6	6	2	2	4	4	4	4	2	2		
SiO ₂	49.82	49.57	49.73	47.77	49.60	48.07	48.07	48.77	1.67	48.51	47.93	1.40	49.27	47.85	1.78	49.82	1.33	47.32	48.48	0.50	52.57	53.47	47.08	1.63	51.94				
TiO ₂	0.10	0.53	0.11	0.68	0.79	0.38	0.44	0.43	0.38	0.60	0.56	0.23	0.55	0.51	0.27	0.19	0.18	0.64	0.33	0.17	0.14	0.16	0.43	0.04	0.16				
Al ₂ O ₃	29.29	26.26	31.17	33.92	30.82	33.40	2.84	30.78	2.51	31.63	32.10	2.01	33.04	32.55	2.25	29.68	1.13	35.31	33.54	2.26	27.13	25.43	33.08	0.56	26.99				
*FeO	2.60	4.87	3.23	2.27	3.73	1.60	1.05	2.10	0.81	2.31	2.59	1.45	3.64	2.05	0.99	2.04	0.55	1.39	2.99	1.17	2.56	3.39	2.15	0.32	3.12				
MgO	3.32	3.14	0.90	1.41	2.07	1.30	0.95	1.29	0.67	2.06	1.55	0.97	1.90	1.32	0.56	2.50	0.50	1.03	1.38	0.86	2.56	2.58	1.41	0.15	3.06				
MnO	0.03	0.00	0.16	0.04	0.07	0.04	0.03	0.03	0.05	0.02	0.03	0.04	0.00	0.02	0.02	0.02	0.02	0.00	0.03	0.04	0.00	0.04	0.02	0.04	0.00				
CaO	0.05	0.08	0.00	0.02	0.07	0.09	0.10	0.15	0.12	0.10	0.08	0.05	0.09	0.12	0.11	0.14	0.16	0.00	0.09	0.06	0.00	0.06	0.04	0.04	0.04				
Na ₂ O	0.09	0.15	0.10	0.51	0.19	0.11	0.08	0.59	0.65	0.26	0.41	0.20	0.53	0.50	0.19	0.19	0.06	0.84	0.78	0.14	0.00	0.00	0.63	0.25	0.20				
K ₂ O	9.42	9.32	10.02	9.45	9.48	10.04	0.61	9.36	0.96	8.95	9.08	0.59	9.73	9.50	0.32	9.66	0.56	9.44	8.14	0.62	9.22	8.92	9.65	0.65	9.14				
Total	94.72	93.92	95.42	96.07	96.82	95.03	2.84	93.50	1.66	94.44	94.33	2.55	98.75	94.42	2.45	94.24	1.49	95.97	95.76	0.71	94.18	94.05	94.49	2.10	94.65				
Numbers of cations on the basis of 22 oxygens																													
Si	6.65	6.76	6.62	6.29	6.52	6.39	6.16	6.58	0.24	6.47	6.42	0.10	6.36	6.40	0.17	6.67	0.14	6.21	6.37	0.08	7.01	7.17	6.32	0.07	6.93				
Al ^{IV}	1.35	1.24	1.38	1.71	1.48	1.61	1.16	1.42	0.24	1.53	1.58	0.10	1.64	1.60	0.17	1.33	0.14	1.79	1.63	0.08	0.99	0.83	1.68	0.07	1.07				
Al ^I	4.60	4.23	4.89	5.27	4.72	5.22	0.39	4.90	0.37	4.97	5.06	0.26	5.03	5.14	0.31	4.68	0.17	5.47	5.20	0.33	4.27	4.02	5.23	0.05	4.24				
Al ^{VI}	3.25	2.99	3.51	3.56	3.24	3.61	0.23	3.48	0.16	3.44	3.48	0.20	3.39	3.54	0.16	3.35	0.05	3.68	3.57	0.25	3.28	3.19	3.55	0.05	3.17				
Ti	0.01	0.05	0.01	0.07	0.08	0.04	0.05	0.04	0.04	0.06	0.04	0.02	0.05	0.05	0.03	0.02	0.02	0.06	0.03	0.02	0.01	0.01	0.04	0.01	0.01				
*Fe ²⁺	0.29	0.56	0.36	0.25	0.41	0.18	0.12	0.24	0.09	0.26	0.29	0.17	0.39	0.23	0.11	0.23	0.06	0.15	0.33	0.13	0.29	0.38	0.24	0.04	0.35				
Mn	0.01	0.00	0.02	0.01	0.01	0.01	0.01	0.00	0.00	0.00	0.00	0.00	0.00	0.00	0.00	0.00	0.00	0.00	0.00	0.00	0.00	0.00	0.00	0.00	0.00				
Mg	0.66	0.64	0.18	0.28	0.41	0.25	0.19	0.26	0.13	0.41	0.31	0.20	0.37	0.26	0.11	0.50	0.09	0.20	0.27	0.17	0.51	0.48	0.28	0.03	0.61				
Sum R ^{VI}	4.22	4.24	4.08	4.17	4.15	4.09	0.05	4.02	0.08	4.17	4.12	0.14	4.20	4.08	0.05	4.10	0.04	4.09	4.20	0.07	4.09	4.07	4.11	0.02	4.14				
Ca	0.01	0.01	0.00	0.01	0.01	0.02	0.01	0.02	0.02	0.01	0.01	0.01	0.01	0.01	0.02	0.02	0.02	0.00	0.01	0.01	0.01	0.01	0.01	0.01	0.01				
Na	0.02	0.04	0.02	0.13	0.05	0.03	0.02	0.16	0.17	0.07	0.11	0.05	0.13	0.13	0.05	0.05	0.02	0.21	0.20	0.03	0.09	0.09	0.17	0.06	0.05				
K	1.61	1.62	1.70	1.59	1.59	1.70	0.07	1.61	0.16	1.52	1.55	0.07	1.60	1.63	0.05	1.65	0.10	1.58	1.37	0.10	1.57	1.53	1.65	0.12	1.55				
t.i.c.	1.65	1.68	1.72	1.74	1.66	1.77	0.05	1.81	0.13	1.61	1.68	0.08	1.75	1.80	0.07	1.74	0.13	1.79	1.59	0.09	1.68	1.64	1.84	0.07	1.62				
Total	13.86	13.91	13.80	13.90	13.80	13.84	0.03	13.81	0.16	13.77	13.79	0.07	13.94	13.86	0.07	13.82	0.10	13.88	13.78	0.09	13.76	13.70	13.94	0.07	13.75				
XMg	0.16	0.15	0.04	0.07	0.10	0.06	0.05	0.06	0.03	0.10	0.08	0.05	0.09	0.06	0.02	0.12	0.02	0.05	0.06	0.04	0.12	0.12	0.07	0.01	0.15				
Fe ²⁺ /	0.31	0.47	0.67	0.47	0.50	0.42	0.22	0.48	0.13	0.39	0.48	0.08	0.51	0.47	0.10	0.32	0.10	0.43	0.55	0.08	0.36	0.44	0.46	0.03	0.37				
(Fe ²⁺ +Mg)	0.77	0.71	0.87	0.87	0.80	0.89	0.06	0.87	0.04	0.84	0.85	0.08	0.82	0.88	0.05	0.82	0.01	0.91	0.86	0.07	0.80	0.79	0.87	0.02	0.77				
(Al ^{VI} +)																													
Fe ²⁺ +Mg)																													
Na/	0.01	0.02	0.01	0.08	0.03	0.02	0.01	0.08	0.09	0.04	0.06	0.03	0.08	0.07	0.03	0.03	0.01	0.12	0.13	0.02	0.05	0.06	0.09	0.04	0.03				
(Na+K)																													
Fe ²⁺ +Mg	0.95	1.20	0.54	0.53	0.82	0.43	0.25	0.50	0.17	0.67	0.60	0.35	0.76	0.49	0.19	0.73	0.05	0.35	0.60	0.30	0.80	0.86	0.52	0.06	0.96				

^aMet., metamorphic (newly formed); 1, older phase; 2, younger phase; Detr., detrital (inherited) grains; x, mean value; SD, standard deviation; n, number of measurements; *, total Fe calculated as FeO or Fe²⁺; t.i.c., total interlayer charge=Na+K+2Ca

Table 4 Chemical compositions of chlorite determined by EMP (weight% and cation numbers)

Sample ^a <i>n</i>	M1			M2			M3		M4		FG9/01		FG10/01		Dz3		Dz5		Dz7		H2		H3			
	2	5	5	3	3	3	3	3	4	4	5	5	5	5	3	3	2	2	4	4	3	3	3	3		
	x	x	SD	x	x	x	SD	x	SD	x	SD	x	SD	x	SD	x	x	x	SD	x	SD	x	SD	x		
SiO ₂	28.57	28.28	1.72	25.99	25.92	27.46	1.08	25.76	0.62	25.54	0.46	26.81	25.26	25.23	1.05	25.29										
TiO ₂	0.01	0.06	0.08	0.02	0.06	0.05	0.06	0.04	0.04	0.06	0.03	0.10	0.04	0.11	0.16	0.02										
Al ₂ O ₃	21.25	20.51	0.84	18.98	18.72	18.38	2.18	20.58	0.55	22.36	0.68	23.43	23.31	20.96	0.56	22.52										
*FeO	22.65	22.64	1.49	31.69	31.27	20.66	0.88	22.23	0.75	26.44	1.16	26.08	26.17	25.55	1.10	27.89										
MgO	16.09	15.00	0.92	9.09	8.64	17.41	1.56	15.11	0.84	11.18	0.91	11.81	11.17	12.26	0.77	10.83										
MnO	0.16	0.13	0.07	0.98	0.76	1.44	0.62	1.81	0.1	0.06	0.02	0.11	0.08	0.05	0.06	0.15										
CaO	0.05	0.07	0.03	0.06	0.03	0.06	0.06	0.33	0.29	0.16	0.05	0.03	0.87	0.13	0.05	0.07										
Na ₂ O	0.03	0.03	0.03	0.02	0.01	0.02	0.01	0.18	0.19	0.19	0.40	0.03	0.07	0.05	0.06	0.04										
K ₂ O	0.06	0.23	0.26	0.14	0.32	0.02	0.02	0	0.01	0.06	0.05	0.27	0.06	0.18	0.27	0.12										
Total	88.87	86.95	3.00	86.97	85.73	85.50	0.73	86.04	0.88	86.05	1.23	88.67	87.03	84.52	0.73	86.93										
Number of cations on the basis of 28 oxygens																										
Si	5.80	5.88	0.16	5.75	5.79	5.86	0.18	5.52	0.11	5.50	0.12	5.57	5.38	5.54	0.18	5.44										
Al ^{IV}	2.20	2.12	0.16	2.25	2.21	2.14	0.18	2.49	0.11	2.50	0.12	2.43	2.62	2.46	0.18	2.56										
Al ^I	5.09	5.03	0.09	4.95	4.95	4.63	0.58	5.19	0.14	5.68	0.11	5.73	5.85	5.42	0.08	5.71										
Al ^{VI}	2.89	2.91	0.12	2.70	2.74	2.48	0.40	2.71	0.13	3.18	0.10	3.30	3.23	2.96	0.23	3.15										
Ti	0.00	0.01	0.01	0.00	0.01	0.01	0.01	0.01	0.01	0.01	0.01	0.02	0.00	0.02	0.03	0.00										
*Fe ²⁺	3.84	3.94	0.18	5.86	5.89	3.69	0.18	3.92	0.14	4.76	0.22	4.53	4.68	4.69	0.23	5.02										
Mn	0.03	0.02	0.01	0.18	0.15	0.26	0.11	0.33	0.02	0.01	0.01	0.02	0.02	0.01	0.01	0.03										
Mg	4.87	4.67	0.42	3.00	2.88	5.54	0.44	4.82	0.26	3.59	0.27	3.65	3.54	4.01	0.29	3.46										
Sum R ^{VI}	11.63	11.55	0.33	11.74	11.67	11.98	0.02	11.79	0.30	11.55	0.16	11.52	11.47	11.69	0.26	11.66										
Ca	0.01	0.01	0.01	0.01	0.01	0.01	0.01	0.08	0.08	0.04	0.01	0.01	0.21	0.03	0.01	0.02										
Na	0.01	0.01	0.01	0.01	0.00	0.01	0.00	0.05	0.04	0.08	0.17	0.01	0.03	0.02	0.03	0.02										
K	0.02	0.06	0.06	0.04	0.09	0.01	0.01	0.00	0.00	0.02	0.01	0.07	0.02	0.05	0.08	0.03										
t.i.c.	0.05	0.09	0.08	0.07	0.11	0.04	0.03	0.21	0.23	0.18	0.17	0.10	0.47	0.13	0.10	0.09										
Sum (Ca+Na+K)	0.04	0.08	0.08	0.06	0.10	0.02	0.02	0.13	0.16	0.14	0.17	0.09	0.26	0.10	0.10	0.07										
Total	19.67	19.63	0.26	19.80	19.77	20.00	0.00	19.92	0.14	19.69	0.13	19.61	19.73	19.79	0.17	19.73										
XMg	0.42	0.40	0.03	0.26	0.25	0.46	0.04	0.41	0.02	0.31	0.02	0.32	0.31	0.34	0.02	0.30										
Fe ²⁺ / (Fe ²⁺ +Mg)	0.44	0.46	0.03	0.66	0.67	0.40	0.03	0.45	0.02	0.57	0.02	0.55	0.57	0.54	0.01	0.59										
Si/(Si+Al ^I)	0.53	0.54	0.01	0.54	0.54	0.56	0.04	0.52	0.01	0.49	0.01	0.49	0.48	0.51	0.01	0.49										
Si+Al ^I +	19.60	19.52	0.20	19.56	19.51	19.72	0.12	19.45	0.31	19.53	0.16	19.48	19.45	19.66	0.29	19.63										
Mg+Fe ²⁺	13.80	13.63	0.36	13.81	13.72	13.86	0.28	13.93	0.23	14.03	0.28	13.91	14.07	14.12	0.47	14.19										

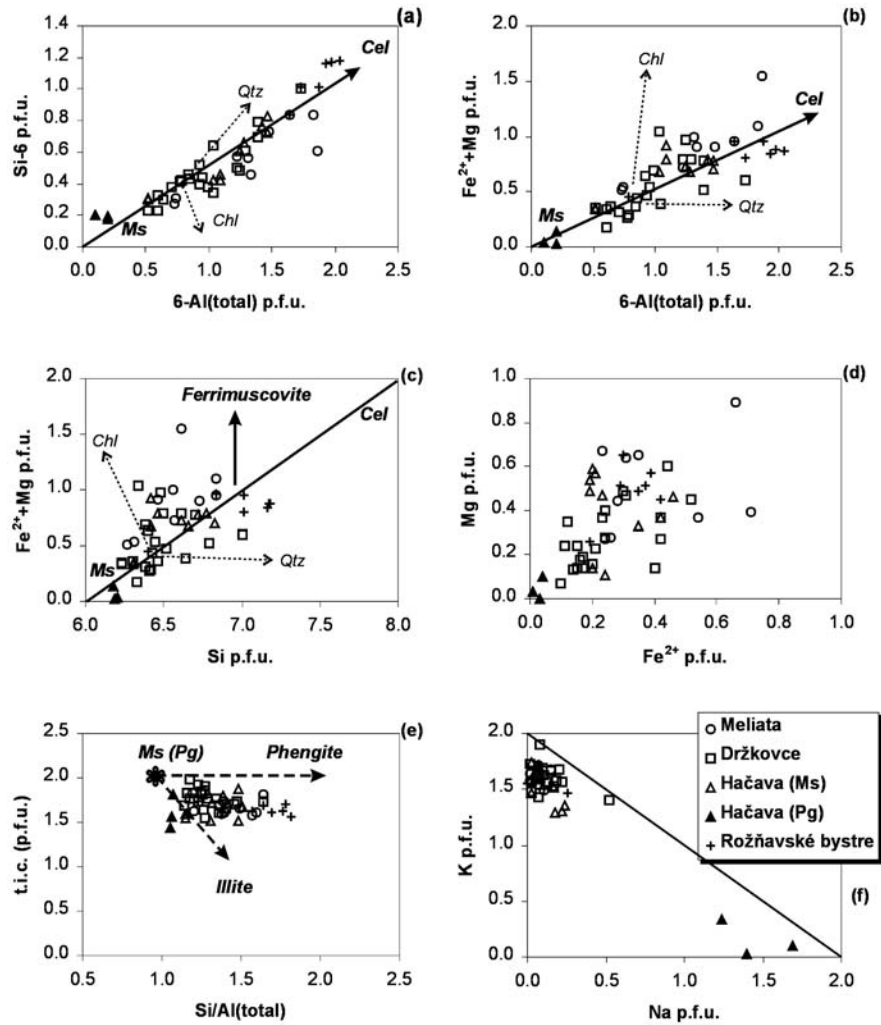
^a *n*, number of measurements; x, mean value; SD, standard deviation; *, total Fe calculated as FeO or Fe²⁺; t.i.c., total interlayer charge=Na+K+2Ca

The K-micas plot mainly along the muscovite–phengite line in Fig. 9e, being slightly shifted in a quasi-parallel way towards the illite field due to small but significant deficits in interlayer charge. This deficit (i.e. total interlayer charge values around 1.7 p.f.u. calculated for 22 oxygens) is characteristic of anchizonal white K-micas (Hunziker et al. 1986; Livi et al. 1997; Merriman and Peacor 1999; Árkai 2002). Figure 9f demonstrates considerable deficiency in the interlayer cation budget for both K- and Na-micas. Some of the K-micas from the Hačava, Držkovce and, partly, also from the Rožňavské Bystre samples show significant Na contents, and all the paragonites from Hačava have considerable K contents (Fig. 9f). Practically no solid solution exists between the Ms–Pg pair at low temperatures (see, for example, Guidotti et al. 1994). Considering also the XRD characteristics (see Fig. 2), it appears likely that in addition to discrete (phengitic) muscovite and paragonite phases, metastable, mixed K–Na-micas also occur in these rocks, with grain sizes near or even below the resolution of the

microprobe. In order to clarify the nature of the mixed K–Na-micas or eventual mixed-layered muscovite(phengite)/paragonite (sensu Livi et al. 1997 or Frey 1969), further TEM and AEM studies are needed.

Although the number of data pairs is rather small (*n*=11), and the data show scattering, the following relations can be observed between KI and white K-mica chemistry in the diagrams of Fig. 10. As can be expected, KI increases (metamorphic grade decreases) with decreasing total interlayer charge (Fig. 10a). There is no obvious correlation between KI and the Na/(Na+K) ratio (Fig. 10b), suggesting that subordinate amounts of discrete paragonite and/or mixed K–Na-micas do not influence the FWHM values of the 10-Å reflection of the dominant illite–muscovite. Figure 10c, d shows that KI increases (apparent grade decreases) with increasing celadonic substitution (with increasing Si and (Mg+Fe²⁺) contents). This relation had originally been established by Esquevin (1969), using indirect (XRD) evidence for celadonic substitution, but it was ques-

Fig. 9a–f Compositional relations of metamorphic dioctahedral white micas. Cation numbers and ratios are calculated from EMP analyses (for explanations, see text). In **a–c**, compositional parameters suggested by Guidotti and Sassi (1998) are used. t.i.c.=total interlayer charge= $K+Na+2Ca$ per formula unit



tioned later on by Hunziker et al. (1986). Árkai et al. (2002) confirmed the effect of celadonic substitution on KI, using a dataset of various lithologies from the Graz Palaeozoic, Eastern Alps, Austria. It is worth mentioning that the Fe/Mg ratio of white micas does not affect the KI, similarly to the samples from the Graz Palaeozoic.

As to the chemical classification scheme of Zane and Weiss (1998), chlorites of the studied samples are tri-trioctahedral type I chlorites, with changing Fe/Mg ratios (see also Table 4). According to the classification of Hey (1954), the chlorites from Meliata metasediments are mainly ripidolite, subordinately brunsvigite and pichnochlorite, and those of the metabasalt are pichnochlorite and ripidolite. In Foster's (1962) system, metasedimentary chlorites fall mainly in the brunsvigite, subordinately in the ripidolite fields, whereas chlorites of metabasalts are mainly in the ripidolite, partly in the brunsvigite fields. After screening the chlorite EMP analyses and excluding those with effects of contamination, the chlorite end-member calculation scheme of Vidal and Parra (2000) shows small but significant (ca. 5 to 25%) sudoitic isomorphous substitutions (Fig. 8).

Figure 11a demonstrates that, disregarding some EMP analyses of chlorites from very fine-grained mix-

tures, the majority of the chlorites shows low (<0.2) total interlayer charge (t.i.c.= $Na+K+2Ca$) values. This indicates that smectitic or illitic impurities, present either as mixed-layers or as intimately intergrown, discrete phases, are insignificant. Increasing ($Al^{VI}-Al^{IV}$) values may be attributed to increasing di-trioctahedral (sudoitic) substitution and/or increasing amounts of smectitic (and illitic) contaminations. Because there is no significant positive correlation between ($Al^{VI}-Al^{IV}$) and t.i.c., the sudoitic substitution may be dominant. Contrasting to the total interlayer charge, apparent octahedral vacancies increase with increasing ($Al^{VI}-Al^{IV}$) (Fig. 11b). This, together with the increase of apparent octahedral vacancies with decreasing sum of octahedral divalent cations (Fig. 11c), unequivocally proves sudoitic substitution in the analysed, predominantly tri-trioctahedral chlorites. Figure 11d shows that the di-trioctahedral substitution plays an important role in chlorites, in addition to the Tschermak' substitution. Most probably, bulk chemical control (Xie et al. 1997; Árkai et al. 2000; Lopez-Munguira et al. 2001; Árkai et al. 2002) and elevated metamorphic pressure (Vidal and Parra 2000) may be the main factors responsible for the considerable sudoitic substitutions.

Fig 10a–d Relations between illite “crystallinity” (KI) and the chemistry of white K-mica

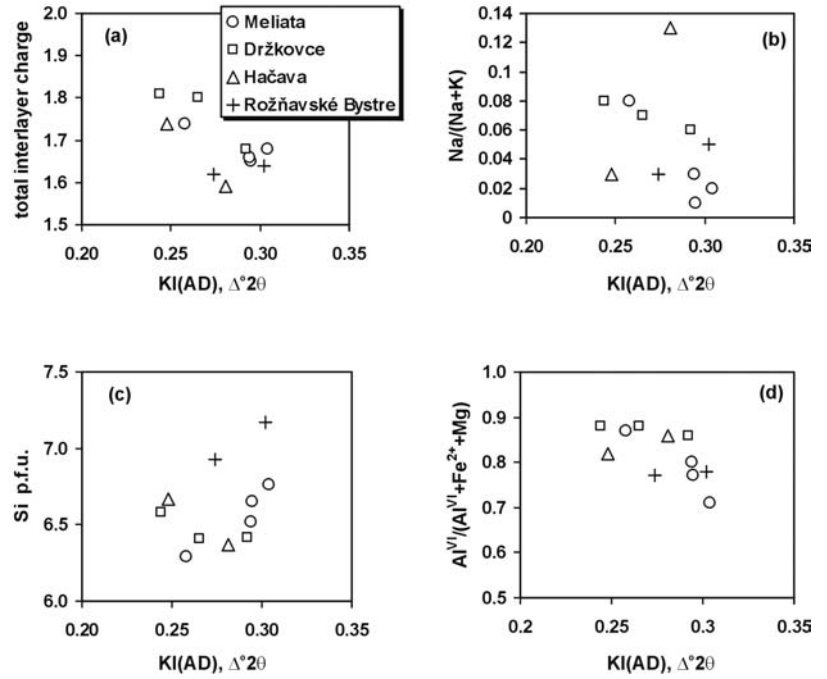


Fig. 11a–d Compositional variation of chlorite (**d** after Zane and Sassi 1998). t.i.c.=total interlayer charge= $K+Na+2Ca$. □=apparent octahedral vacancy= $20-\Sigma$ octahedral cations per formula unit. Arrows show trends of *TK* Tschermak’s, and *AM* dioctahedral (sidoitic) substitutions (after Zane and Sassi 1998), where $\Delta=Al^{IV}-(Al^{VI}+2Ti)$

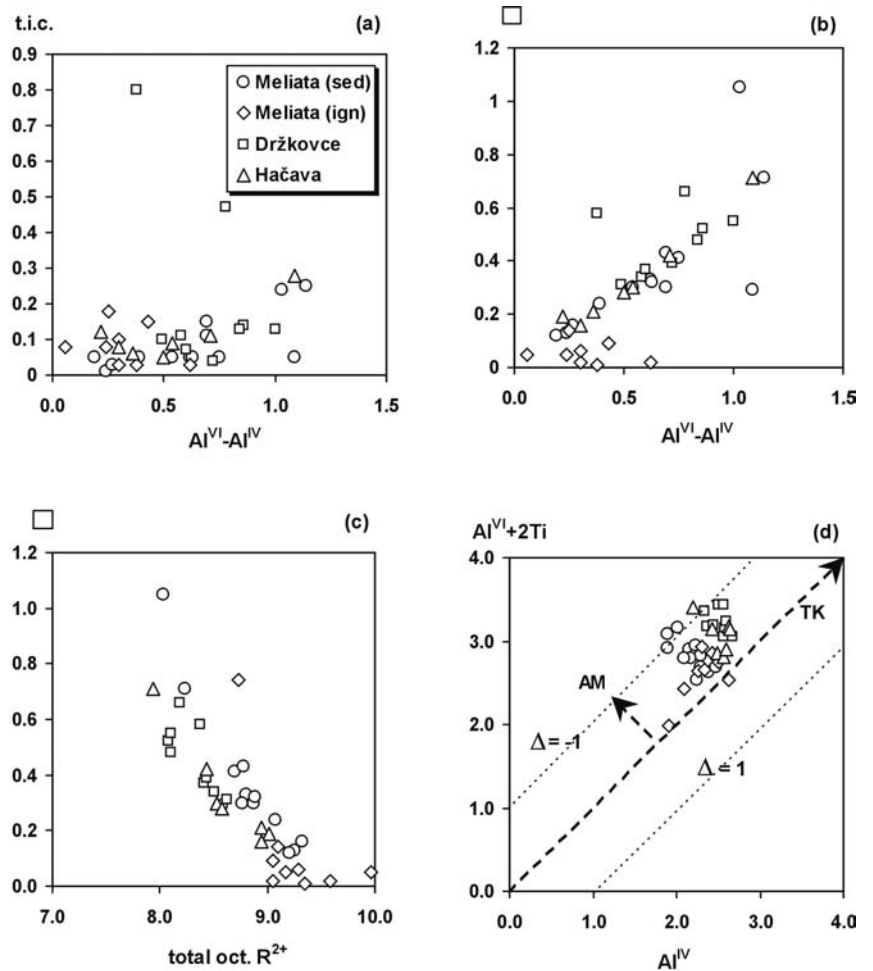


Table 5 Peak temperature estimates of metamorphism in °C, calculated by chlorite–Al^{IV} thermometry (*n* number of samples, *SD* standard deviation)

Thermometer	Statistical parameters	Meliata (metasediments)	Meliata (metabasalts)	Držkovce	Hačava
Cathelineau and Nieva (1985)	Mean	282	315	348	342
	SD	38	35	18	25
	<i>n</i>	13	10	9	7
	Min.	242	246	315	299
	Max.	337	362	368	363
Kranidiotis and McLean (1987)	Mean	290	298	327	325
	SD	22	25	13	17
	<i>n</i>	13	10	9	7
	Min.	256	248	304	292
	Max.	335	338	346	345
Jowett (1991)	Mean	297	318	351	349
	SD	29	35	18	25
	<i>n</i>	13	10	9	7
	Min.	249	248	321	299
	Max.	350	365	376	372
Zang and Fyfe (1995)	Mean	229	258	264	263
	SD	18	20	11	16
	<i>n</i>	13	10	9	7
	Min.	191	219	245	232
	Max.	248	286	277	277

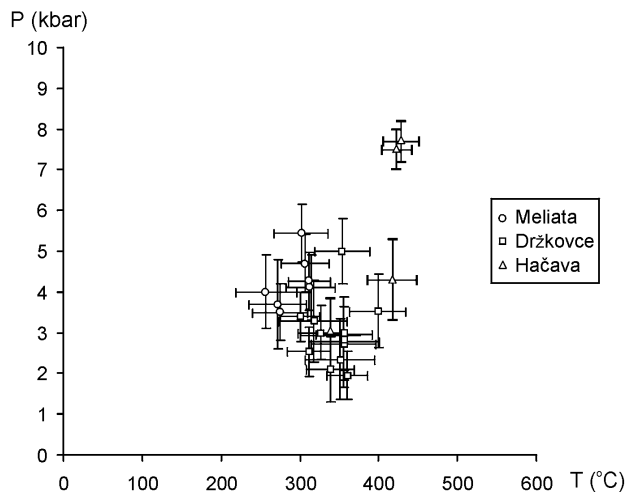


Fig. 12 P–T estimates of metamorphism calculated by the method of Vidal and Parra (2000). Error bars correspond to 1 σ standard deviation. For further explanation, see the text

Table 5 summarizes the metamorphic temperatures calculated by the chlorite–Al^{IV} thermometer of Cathelineau and Nieva (1985). Note that similar T values were obtained also with the modified versions of this thermometer by Kranidiotis and McLean (1987) and Jowett (1991), whereas the calibration of Zang and Fyfe (1995) gave significantly lower, unrealistic results. The mean T values are around 300 °C for the Meliata locality, and about 340 °C for the Držkovce and Hačava localities. Both the trend of increasing T and also the absolute values are in fairly good agreement with the estimates obtained from the KI values characteristic of high-temperature anchizonal metamorphism.

Figure 12 and Table 6 summarize the P–T results obtained using the chlorite–white mica thermobarometer of

Table 6 Pressure and temperature estimates calculated by white mica–chlorite thermometry of Vidal and Parra (2000) (*n* number of samples, *SD* standard deviation)

Locality	Statistical parameters	T (°C)	P (kbar)
Meliata metasediments (M1, M2)	Mean	288	4.3
	SD	22	0.7
	<i>n</i>	5	5
	Min.	257	3.5
	Max.	312	5.4
Držkovce (Dz3, Dz5, Dz7)	Mean	342	3.1
	SD	27	0.8
	<i>n</i>	13	13
	Min.	300	1.9
	Max.	399	5.0
Hacava (H3)	Mean	378	3.6
	SD		
	<i>n</i>	2	2
	Min.	339	2.9
	Max.	417	4.3
Hacava (H2)	Mean	425	7.6
	SD		
	<i>n</i>	2	2
	Min.	423	7.5
	Max.	428	7.7

Vidal and Parra (2000). They were constrained by the intersection of four independent equilibria. The results of average P–T estimates correspond to the INTERSX output. The temperature and pressure standard deviations lie within 10–40 °C (mean value=31 °C) and 260–1,100 bar (mean value=750 bar) respectively. The highest standard deviations may witness disequilibrium between the chlorite and white K-mica used to estimate the P–T conditions. However, the P–T conditions for the pairs showing the highest and lowest standard deviations (highest and

Table 7 K–Ar isotopic data of the <2 μm grain-size white K-mica-rich fraction samples

Sample	K (%)	$^{40}\text{Ar}(\text{rad})$ ($10^{-5} \text{ cm}^3/\text{g}$)	$^{40}\text{Ar}(\text{rad})$ (%)	Age $\pm\sigma^a$ (Ma)
M1	3.507	1.813	73.0	128.3 \pm 5.0
M2	4.394	2.376	71.9	134.0 \pm 5.2
M3	2.330	1.506	67.6	159.1 \pm 6.2
M4	3.517	2.553	85.1	177.7 \pm 6.8
Dz1	6.499	3.021	81.9	115.8 \pm 4.5
Dz3	5.831	2.964	87.6	126.2 \pm 4.9
Dz5	5.998	3.462	83.8	142.7 \pm 5.7
Dz7	5.520	3.338	86.3	149.2 \pm 5.7
Rb-7	2.496	1.277	63.4	127.0 \pm 5.1
Rb3	5.097	2.943	78.5	142.7 \pm 5.6
Rb4	3.517	1.737	80.3	122.8 \pm 4.8
Rb5	4.905	3.159	82.8	158.5 \pm 6.0
H2	3.882	2.277	86.6	144.9 \pm 5.7
H3	6.433	3.582	90.6	137.8 \pm 5.4
H11	3.303	1.830	81.6	137.2 \pm 5.4
H12	3.659	2.152	85.0	145.3 \pm 5.5

^a Calculated using atomic decay constants of Steiger and Jäger (1977)

lowest scatter among the intersections of independent equilibria) are not significantly different. It is thus believed that the standard deviations obtained in the present study are compatible with the assumption of equilibrium at local (microscopic) scale.

For the Meliata metapelites the calculated temperature and pressure values scatter in the ranges of 257–312 °C and 3.5–5.4 kbar, giving averages of 288 \pm 22 °C and 4.3 \pm 0.7 kbar. In the case of the Držkovce samples, higher but strongly scattering temperatures (300–399 °C, with a mean value of 342 \pm 27 °C), and also strongly scattering but lower pressure values (1.9–5.0, average is 3.1 \pm 0.8 kbar) were obtained, as compared to the Meliata rocks. Two Hačava samples gave rather distinct P–T intervals. P–T values of sample H3 are 339–417 °C (mean of 378 °C) and 2.9–4.3 kbar (average of 3.6 kbar), these being somewhat higher than the P–T values of the Držkovce samples. For sample H2, relatively high T (425 °C) and P (7.6 kbar) conditions were obtained.

K–Ar geochronology of white K-micas

The age of the blueschist facies metamorphism of the Meliata unit is about 165–155 Ma (Maluski et al. 1993, Dallmayer et al. 1993, Faryad and Henjes-Kunst 1997). Table 7 summarizes the new K–Ar isotope data for white K-mica-rich, <2 μm grain-size fractions of selected, very low-grade samples. The K–Ar data obtained for different samples scatter in the wide range of 177–116 Ma, suggesting the presence of different generations of white K-micas. Samples from the Meliata locality, the metamorphic temperature of which was the lowest, yielded the largest scatter in age values. The older ages of 177.7 \pm 6.8 and 159.1 \pm 6.2 Ma were obtained for samples M3 and M4 which contain relatively coarse-grained, low-Si mica, and the younger ages of 134.0 \pm 5.2 and

128.3 \pm 5.0 Ma for fine-grained samples (M1 and M2) with high-Si mica. The youngest dates of 134 and 128 Ma can be interpreted as the age of very low-grade metamorphism, whereas the oldest dates reflect the presence of an older, detritic mica component.

The K–Ar data for the Držkovce locality yielded two groups of ages: 149 and 143 Ma for samples Dz7 and Dz5, and 126 and 116 Ma for samples Dz3 and Dz1. Both ages are younger than the blueschist facies metamorphism and probably reflect very low-grade metamorphic events in these rocks, documented by illite and chlorite “crystallinity” indices.

Samples from the Hačava locality yielded ages in the narrow range of 137–145 Ma. The older ages (144–145 Ma) come from dark calcite- and graphite-rich samples which contain paragonite rimmed by phengite, whereas the younger age (137 Ma) was obtained from an overlying pelitic rock.

Three different ages (127–122, 142 and 158 Ma) were obtained on fine, white mica fractions of mylonitised phyllites from the Rožňavské Bystre locality. The first two ages are comparable with those from the Držkovce locality. The last age of 158 Ma probably reflects the presence of blueschist facies, white mica relic.

Discussion

Figure 13 shows the most probable P–T–t paths constructed for the retrogressed (mylonitised) blueschist facies metasediments of Rožňavské Bystre (Rb), and the prograde anchizonal series of the localities Meliata (M), Držkovce (Dz) and Hačava (H). When comparing the temperature estimates, fairly good agreement is found between the results obtained by various methods. Illite Kübler-index (“crystallinity”) and chlorite “crystallinity” data revealed upper anchizonal conditions with T estimates of ca. 270–350 °C, the Meliata rocks showing lower, the other groups higher temperatures. These results agree with the T estimates based on the chlorite–Al^{IV} thermometers of Cathelineau and Nieva (1985), and Jowett (1991), indicating 280–315 °C for the Meliata and 340–350 °C for the Držkovce and Hačava samples (Table 5). Moreover, these temperature estimates practically coincide with those obtained for the Meliata and Držkovce groups by the chlorite–white mica thermobarometer of Vidal and Parra (2000). This latter method gave higher T estimates for the Hačava samples. The surprisingly good agreement between the T estimates by the various methods suggests that the kinetic factors of low-T metamorphism of the Meliata unit may be comparable to those terrains for which the “crystallinity” scales and the chlorite–Al^{IV} thermometers were calibrated. Yet, local near-equilibrium states at a microscale of several hundreds to thousands of micrometres have been attained, even if the rock as a bulk represented disequilibrium.

For the Meliata locality (where no paragonite or mixed K–Na-mica were found), semiquantitative P esti-

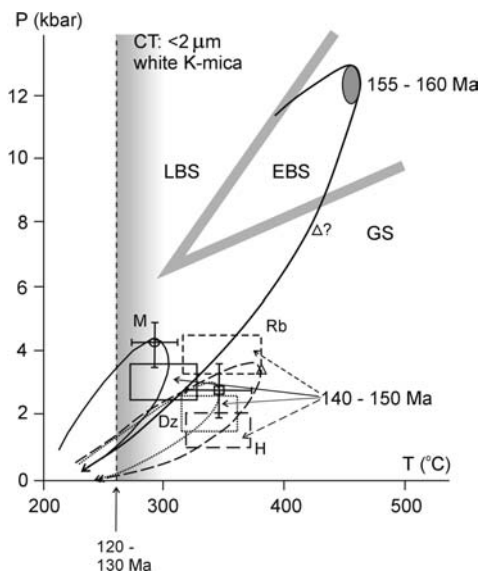


Fig. 13 P–T diagram indicating the exhumation path (mylonitisation and retrogression) of blueschists and the P–T trajectories of very low-grade metamorphism of sedimentary sequences in the Meliata unit. Dates of 155–160 Ma correspond to blueschist facies metamorphism (Maluski et al. 1993; Dallmayer et al. 1993; Faryad and Henjes-Kunst 1997). The age interval of 140–150 Ma is interpreted to date the very low-grade progressive metamorphism of pelitic sequences and retrogression of blueschist facies rocks of the Meliata unit. The interval of 120–130 Ma is tentatively related to cooling of the sequences below the closure temperature of the $<2\ \mu\text{m}$ white K-micas (ca. $260\ ^\circ\text{C}$). Boxes represent the uncertainties of P and T estimations using the illite and chlorite “crystallinity”, chlorite–Al^{IV} thermometric, and white K-mica *b* geobarometric methods. In the case of the Držkovce, Hačava, and Rožňavské Bystre samples, these pressure ranges should be considered as minimum estimates (see also the text). Symbols with error bars expressing $\pm 1\sigma$ standard deviation show average P–T data obtained by chlorite–white mica thermobarometry (Vidal and Parra 2000). *M*, continuous line, circle Meliata; *Dz*, dotted line, square Držkovce; *H*, dashed line, triangle Hačava; *Rb*, finely dashed line Rožňavské Bystre. Other abbreviations: *LBS* lawsonite blueschist, *EBS* epidote blueschist, *GS* greenschist facies. The CT-closure temperature of the radiogenic Ar system in the $<2\ \mu\text{m}$ grain-size fraction of illite–muscovite is after Hunziker et al. (1986)

mates based on white K-mica *b* geobarometry (Sassi 1972; see also Guidotti and Sassi 1986) are lower by ca. 1–1.5 kbar than the P estimates obtained by chlorite–white mica thermobarometry (Vidal and Parra 2000). The reasons for this discrepancy are not known at present. Perhaps the linear extrapolation of the white K-mica *b* isopleths to lower temperatures may be an oversimplified approximation, and/or the lack of limiting mineral assemblages may increase the uncertainties of white mica *b* geobarometry. The Držkovce samples are characterised by higher T and lower P than the Meliata samples. The discrepancy between the P estimates obtained by the two above-mentioned methods is similar to that found for the Meliata sample group, although paragonite is present in the Držkovce samples which, according to Guidotti and Sassi (1976), should cause a decrease of the *b* values and consequently, the P estimates

may be regarded as minimum pressure values. With increased paragonite content, as in the case of the Hačava samples, the discrepancy between the P estimates by the two methods are the largest. Here the P values obtained by the chlorite–white mica method of Vidal and Parra (2000) seem to be reliable, whereas the *b* method underestimates the pressure conditions. It is worth mentioning that the imprint of an earlier, higher-P event (inferred from the white K-mica *b* data) has been substantiated also by chlorite–white mica thermobarometry. In conclusion, the thermobarometric data indicate that metamorphism of the various localities/formations proceeded along varying P/T gradients.

In Fig. 13 the time relations of metamorphism are also shown, as deduced from the K–Ar age data of the $<2\ \mu\text{m}$ grain-size, white K-mica-rich fractions. Of course, the $<2\ \mu\text{m}$ grain-size fraction of illite–muscovite-rich parts of the metaclastic rocks does not represent a homogeneous white-mica generation. In addition to the predominant, newly formed (metamorphic) micas, fine fragments of older (inherited) detrital flakes may occur. Consequently, the interpretation of K–Ar age data needs special care. Supposing an effective heating time of 10 ± 5 Ma, total isotopic resetting of the $<2\ \mu\text{m}$ grain-size illite–muscovite fraction is achieved at $260\pm 20\ ^\circ\text{C}$ (Hunziker et al. 1986). Therefore, this T value is generally regarded as the closure temperature of these fine-grained micas. According to Árkai et al. (1995a), chemical equilibrium in the Palaeozoic and Mesozoic of the Bükkium, NE Hungary was approached (but not completely achieved) at upper anchizonal and epizonal conditions. Small (ca. 5%) but systematic differences between the K–Ar ages of $<2\ \mu\text{m}$, white K-mica fractions of terrigenous metaclastic rocks and metatuffs suggest that the effects of inherited old micas are present even in epizonal rocks. The differences between the peak temperature of metamorphism (ca. $280\text{--}350\ ^\circ\text{C}$) and the closure temperature of the K–Ar system ($\sim 260\ ^\circ\text{C}$) resetting during cooling may result in somewhat younger ages than the actual age of peak conditions. On the other hand, even small proportions of detrital micas in the $<2\ \mu\text{m}$ grain-size illite–muscovite fraction may affect the resultant K–Ar system, producing older ages than that of the metamorphic peak. Considering these two contrasting effects which may modify the age values in opposite ways, one may suppose that the K–Ar data in Table 7 (displayed also in Fig. 13) can be related to the actual age of peak conditions of the very low-grade sedimentary mélange, as a very rough approximation.

By contrast, K–Ar dates from the mylonites record a retrograde episode in the blueschist facies metapelites. Geological observations, together with metamorphic conditions and their age relations, point to complex tectonic imbrication, mixing of blueschist facies and very low-grade (anchizonal) metamorphic series (tectonic slices, lenses) at relatively shallow (10–20 km) crustal levels in an accretionary wedge. The studied mélange is similar in its structural, petrological and tectonic aspects to those observed in various accretionary complexes (see, for example, Cowan 1985; Goodge 1995).

Cretaceous deformation and metamorphism (100–90 Ma), which were significant in the surrounding (and underlying) Gemericum as well as in the Veporicum and in the Bükk unit of the Western Carpathians (Kovács et al. 1986; Maluski, et al. 1993; Árkai et al. 1995a; Kovacik et al. 1997), had no or only minimal effect on the Meliata unit. With the exception of a low-temperature overprint at ~90 Ma, deduced from Ar–Ar spectra (Faryad and Henjes-Kunst 1997), there is no geochronological evidence of Cretaceous tectonic activity. This event probably led only to brittle deformation of the rocks in this unit.

Conclusions

1. The sedimentary matrix of the Meliata mélange and associated metabasalts in the inner Western Carpathians, Slovakia experienced prograde, high-T anchizonal (ca. 280–350 °C) regional metamorphism. The grade of metamorphism is somewhat lower at the type locality of the village Meliata than at the other localities studied. High-T anchizonal conditions prevailed also during the mylonitic retrogression of the blueschist facies phyllites (Rožňavské Bystre).
2. White micas are characterised by a slight deficiency of the interlayer charge. Variations in the chemistry of white K-micas follow the main trend of Tschermak'-type (or celadonic) isomorphic substitution. Illite "crystallinity" increases (i.e. apparent metamorphic grade decreases) with decreasing total interlayer charge and increasing celadonic substitution, whereas Na/K and Fe/Mg ratios do not affect the KI values considerably.
3. In general, smectitic and/or illitic impurities (mixed layers or finely intergrown, discrete phases) are insignificant in chlorites. Chemical relations of chlorites show that dioctahedral (sudaotic) substitution plays an important role in addition to the Tschermak' and FeMg₁substitutions.
4. Illite and chlorite "crystallinity" data are in fairly good agreement with each other, and also with the results of chlorite–Al^{IV}thermometry and chlorite–white mica thermobarometry.
5. Discrete paragonite and "mixed" white K-Na-mica phases, being present in subordinate quantities, do not appreciably modify the illite "crystallinity" values, and consequently the estimates on metamorphic grade. On the other hand, *b*values of white K-micas provide only minimum pressure estimates in samples containing also paragonite and/or "mixed" white K-Na-mica phases.
6. Accordingly, the minimum pressure of prograde anchizonal metamorphism varied between ca. 3 and 1.5 kbar, that of the retrogression of blueschist facies metapelites being about 4 kbar. Based on the results of chlorite–white mica thermobarometry (Vidal and Parra 2000), the pressure of prograde low-T metamorphism may have varied between ca. 2.5 and 5 kbar,

locally (at Hačava) with indication of an earlier, ca. 7–8 kbar event. The P–T estimates for the different localities suggest variable thermobaric conditions in the accretionary wedge.

7. Prograde anchizonal metamorphism and retrogression of blueschist facies metapelites occurred between ca. 150 and 120 Ma, with a thermal peak in the anchizonal sequences at around 140–145 Ma. Thus, the very low-grade metamorphism of the Meliata sedimentary pile was younger than the 160–155 Ma old, subduction-related blueschist facies metamorphism, and considerably older than the Cretaceous (ca. 100–90 Ma) metamorphism of the footwall Gemer and surrounding Vepor Palaeozoic units (Slovakia), and of the Palaeozoic and Mesozoic formations of the Bükk unit (NE Hungary).

Acknowledgements The authors thank the technical co-workers of the Laboratory for Geochemical Research, Hungarian Academy of Sciences, Budapest for their assistance. Thus, thanks are due to Mrs. O. Komoróczy, Cs.M. Sándor, Ms. K. Temesvári and N. Keresztes for XRD work, and to Ms. N Szász for preparing polished thin sections. Prof. G. Hoinkes is thanked for making available facilities for microprobe analysis in the Institute of Mineralogy and Petrology, University of Graz. The authors are indebted to Prof. B. Goffé, Prof. T. Theye and Prof. M. Raith for critically reviewing, correcting and improving the manuscript. The present work was financially supported by the Hungarian Scientific Research Fund (OTKA), Budapest, programs nos. T-035050/2001–2004 to P.Á and T-029897/1999–2002 to K.B.

References

- Árkai P (2002) Phyllosilicates in very low-grade metamorphism: transformation to micas. In: Mottana A, Sassi FP, Thompson JB, Guggenheim S (eds) *Micas: crystal chemistry and metamorphic petrology*. Mineralogical Society of America, Blacksburg, Virginia, *Rev Mineral Geochem* 46:463–478
- Árkai P, Kovács S (1986) Diagenesis and regional metamorphism of Aggtelek–Rudabánya Mountains (Northern Hungary). *Acta Geol Hung* 29:349–373
- Árkai P, Sassi R, Zirpoli G (1991) On the boundary between the low- and very low-grade South-Alpine basement in Pustertal: X-ray characterization of white mica in metapelites between Dobbiaco (Toblach, Italy) and Leiten (Austria). *Mem Sci Geol Padova* 63:293–304
- Árkai P, Balogh K, Dunkl I (1995a) Timing of low-temperature metamorphism and cooling of the Paleozoic and Mesozoic formations of the Bükkium, innermost Western Carpathians, Hungary. *Geol Rundsch* 84:334–344
- Árkai P, Sassi FP, Sassi R (1995b) Simultaneous measurements of chlorite and illite crystallinity: a more reliable geothermometric tool for monitoring low- to very low-grade metamorphism in metapelites. A case study from Southern Alps (NE. Italy). *Eur J Mineral* 7:1115–1128
- Árkai P, Mata MP, Giorgetti G, Peacor DR, Tóth M (2000) Comparison of diagenetic and low-grade metamorphic evolution of chlorite in associated metapelites and metabasites: an integrated TEM and XRD study. *J Metamorph Geol* 18:531–550
- Árkai P, Fenninger A, Nagy G (2002) Effects of lithology and bulk chemistry on phyllosilicate reaction progress in the low-T metamorphic Graz Paleozoic, Eastern Alps, Austria. *Eur J Mineral* 14:673–686
- Berman RG (1991) Thermobarometry using multi-equilibrium calculations. A new technique, with petrologic applications. *Can Mineral* 29:835–855

- Cathelineau M, Nieva D (1985) A chlorite solid solution geothermometer. The Los Azufres (Mexico) geothermal system. *Contrib Mineral Petrol* 91:235–244
- Cowan DS (1985) Structural styles in Mesozoic and Cenozoic mélanges in the Western Cordillera of North-America. *Geol Soc Am Bull* 96:451–462
- Dallmeyer RD, Neubauer H, Fritz H, Putiš M (1993) Variscan vs. Alpine tectonothermal evolution within the Eastern Alps and Western Carpathians, Austria-Slovakia. In: Proc PAEWCR Conf, September 1993, Stará Lesná, Slovakia. *Geol Carpathica* 44:255–256
- Esquevin J (1969) Influence de la composition chimique des illites sur leur cristallinité. *Bull Centre Res Pau-SNPA* 3:147–153
- Faryad SW (1995) Phase petrology of mafic blueschists of the Meliata Unit (West Carpathians) – Slovakia. *J Metamorph Geol* 13:432–448
- Faryad SW (1997) Lithology and metamorphism of the Meliata unit high-pressure rocks. In: Grecula P, Hovorka D, Putiš M (eds) Geological evolution of the Western Carpathians. *Mineralia Slovaca Corp Geocomplex as Geol Surv Slovak Republic*, Bratislava, pp 131–144
- Faryad SW (1998) Vysokotlakové metamorfované horniny meliatskej jednotky versus príkrov Bôrky; ich korelácia s obliakmi modrých bridlic v zlepenoch klapskej jednotky bradlového pásma – diskusia. *Miner Slovaca* 30:235–240
- Faryad SW, Dianiška I (1999) Metagabbro with relic richterite from the Permian evaporite melange near Bohúňovo (Western Carpathians). In: 77th DMG Conf MinWien 1999, Vienna. *Beih Eur J Mineral* 11:68
- Faryad SW, Henjes-Kunst F (1997) K-Ar and Ar-Ar age constraints of the Meliata blueschist facies rocks, the Western Carpathians (Slovakia). *Tectonophysics* 280:141–156
- Foster MD (1962) Interpretation of the composition and a classification of the chlorites. *US Geol Surv Prof Pap* 414/A:1–33
- Frey M (1969) A mixed-layer paragonite/phengite of low-grade metamorphic origin. *Contrib Mineral Petrol* 14:63–65
- Frey M (1987) Very low-grade metamorphism of clastic sedimentary rocks. In: Frey M (ed) *Low temperature metamorphism*. Blackie, Glasgow, pp 9–58
- Frey M, Niggli E (1972) Margarite, an important rock-forming mineral in regionally metamorphosed low-grade rocks. *Naturwissenschaften* 59:214–215
- Goode JW (1995) Pre Middle Jurassic accretionary metamorphism in the southern Klamath Mountains of northern California, USA. *J Metamorph Geol* 13:93–110
- Guidotti CV, Sassi FP (1976) Muscovite as a petrogenetic indicator mineral in pelitic schists. *N Jb Miner Abh* 127:97–142
- Guidotti CV, Sassi FP (1986) Classification and correlation of metamorphic facies series by means of muscovite data from low-grade metapelites. *N Jb Miner Abh* 153:363–380
- Guidotti CV, Sassi FP (1998) Petrogenetic significance of Na-K white mica mineralogy: recent advances for metamorphic rocks. *Eur J Mineral* 10:815–854
- Guidotti CV, Sassi FP, Blenkoe JG, Selverstone J (1994) The paragonite-muscovite solvus. I. P-T-X limits derived from the Na-K compositions of natural, quasibinary paragonite-muscovite pairs. *Geochim Cosmochim Acta* 58:2269–2275
- Hey MH (1954) A new review of the chlorites. *Mineral Mag* 30:277–292
- Horváth P (2000) Metamorphic evolution of gabbroic rocks of the Bódva Valley ophiolite complex, NE Hungary. *Geol Carpathica* 51:121–129
- Hovorka D, Ivan P, Jaroš J, Kratochvíl M, Reichwalder P, Rojkovič I, Spišiak J, Turanová L (1985) Ultramafic rocks of the Western Carpathians, Czechoslovakia. *Geol Inst Dionýz Štúr*, Bratislava, pp 1–258
- Hunziker JC, Frey M, Clauer N, Dallmeyer RD, Friedrichsen H, Flehmig W, Hochstrasser K, Roggwiler P, Schwander H (1986) The evolution of illite to muscovite: mineralogical and isotopic data from the Glarus Alps, Switzerland. *Contrib Mineral Petrol* 92:157–180
- Ivan I, Kronome B (1996) Predmetamorfny charakter a geodynamické prostredie vzniku vysokotlakovo metamorfovaných bázitov meliatskej jednotky na lokalitách Radzim, Bôrka, Hačava a Rudník. *Miner Slovaca* 28:26–37
- Jowett EC (1991) Fitting iron and magnesium into the hydrothermal chlorite geothermometer. In: Program Abstr Vol GAC/MAC/SEG Joint Annu Meet, 27–29 May 1991, Toronto. Vol 16, p A62
- Kisch HJ (1983) Mineralogy and petrology of burial diagenesis (burial metamorphism) and incipient metamorphism in clastic rocks. In: Larsen G, Chilingar GV (eds) *Diagenesis of sediments and sedimentary rocks 2*. Elsevier, Amsterdam, pp 289–493
- Kisch HJ (1987) Correlation between indicators of very low-grade metamorphism. In: Frey M (ed) *Low temperature metamorphism*. Blackie, Glasgow, pp 227–300
- Kováč A, Svingor E, Grecula P (1986) Rb-Sr isotope ages of granitoid rocks from the Spišsko gemerské rudohorie Mts. *Miner Slovaca* 18:1–14
- Kováčik M, Král J, Maluski H (1997) Alpine reactivation of the southern Veporicum basement: metamorphism, ⁴⁰Ar/³⁹Ar dating, geodynamic model and correlation aspects with Eastern Alps. In: Grecula P, Hovorka D, Putiš M (eds) Geological evolution of the Western Carpathians. *Mineralia Slovaca Corp – Geocomplex a.s. – Geol Surv Slovak Republic*, Bratislava, pp 43–65
- Kozur H, Mock R (1996) New paleogeographic and tectonic interpretations in the Slovakian Carpathians and their implications for correlations with the Eastern Alps. Part I. Central Western Carpathians. *Miner Slovaca* 28:151–174
- Kranidiotis P, MacLean WH (1987) Systematics of chlorite alteration at the Phelps Dodge massive sulfide deposit, Matagami, Quebec. *Econ Geol* 82:1898–1911
- Kübler B (1967) La cristallinité de l'illite et les zones tout à fait supérieures du métamorphisme. In: Proc Coll Étages Tectoniques, 1966, Neuchâtel. A La Baconnière, Neuchâtel, pp 105–121
- Kübler B (1990) "Cristallinité" de l'illite et mixed-layers: brève révision. *Schweiz Mineral Petrogr Mitt* 70:89–93
- Leško B, Varga I (1980) Alpine elements in the Western Carpathians structure and their significance. *Miner Slovaca* 12:97–130
- Livi KJT, Veblen DR, Ferry JM, Frey M (1997) Evolution of 2:1 layered silicates in low-grade metamorphosed Liassic shales of Central Switzerland. *J Metamorph Geol* 15:323–344
- Lopez-Munguira A, Nieto F, Morata D (2001) Chlorite composition controlled by whole-rock chemistry: a DRX-EMP/HRTEM-AEM study in Cambrian basaltic rocks from the Ossa Morena Zone, SW Spain. *J Conf Abstr* 6:236
- Mahel' M (1986) Geological structure of the Czechoslovak Carpathians. Paleozoic units. Veda, Bratislava, pp 1–496
- Maluski H, Rajlich P, Matte Ph (1993) ⁴⁰Ar/³⁹Ar dating of the Inner Carpathian Variscan Basement and Alpine mylonitic overprinting. *Tectonophysics* 223:313–337
- Mazzolli G, Vozárová A (1998) Subduction related processes in the Bôrka nappe (Inner Western Carpathians): a geochemical and petrological approach. In: Rakús M (ed) *Geodynamic development of the Western Carpathians*. Dionýz Štúr Publ, 89–106
- Mello J (1993) Meliatikum: geologický vývoj, postavenie a vzťah k okolitým jednotkám. Manuscript Archív GS, Bratislava, pp 1–39
- Mello J, Elečko J, Pristaš J, Reichwalder P, Snopko L, Vass D, Vozárová A (1996) Geologická mapa slovenského krasu, mierka 1:50 000. Geological Survey, Bratislava
- Merriman RJ, Frey M (1999) Patterns of very low-grade metamorphism in metapelitic rocks. In: Frey M, Robinson D (eds) *Low-grade metamorphism*. Blackwell, Oxford, pp 61–107
- Merriman RJ, Peacor DR (1999) Very low-grade metapelites: mineralogy, microfabrics and measuring reaction progress. In: Frey M, Robinson D (eds) *Low-grade metamorphism*. Blackwell, Oxford, pp 10–60
- Mock R (1978) Niektoré nové poznatky o južnej časti Západných Karpát. In: Vozár J (ed) *Paleogeografický vývoj Západných Karpát*. Geologický ústav Dionýza Štúra, Bratislava, pp 322–341

- Odin GS et al. (1982) Interlaboratory standards for dating purposes. In: Odin GS (ed) Numerical dating in stratigraphy. Wiley, Chichester, pp 123–150
- Padan A, Kisch HJ, Shagam R (1982) Use of the lattice parameter b_0 of the dioctahedral illite/muscovite for the characterization of P/T gradients of incipient metamorphism. *Contrib Mineral Petrol* 79:85–95
- Sassi FP (1972) The petrologic and geologic significance of the b_0 value of potassic white micas in low-grade metamorphic rocks. An application to the Eastern Alps. *Tschermak's Mineral Petrogr Mitt* 18:105–113
- Steiger RH, Jäger E (1977) Subcommittee on geochronology: convention on the use of decay constants in geo- and cosmochronology. *Earth Planet Sci Lett* 12:359–362
- Vidal O, Parra T (2000) Exhumation paths of high-pressure metapelites obtained from local equilibria for chlorite-phengite assemblages. *Geol J* 35:139–161
- Vidal O, Parra T, Trotet F (2001) A thermodynamic model for Fe-Mg aluminous chlorite using data from phase equilibrium experiments and natural pelitic assemblages in the 100–600 °C, 1–25 kbar P-T range. *Am J Sci* 301:557–592
- Xie X, Byerly GR, Ferrel RE Jr (1997) IIB trioctahedral chlorite from the Barberton greenstone belt: crystal structure and rock composition constraints with implications to geothermometry. *Contrib Mineral Petrol* 126:275–291
- Zane A, Sassi R (1998) New data on metamorphic chlorite as a petrogenetic indicator mineral, with special regard to greenschist-facies rocks. *Can Mineral* 36:713–726
- Zane A, Weiss Z (1998) A procedure for classifying rock-forming chlorites based on microprobe data. *Rend Fis Acc Lincei Ser* 9(9):51–56
- Zang W, Fyfe WS (1995) Chloritisation of the hydrothermally altered bedrock at the Igarape Bahia gold deposit, Carajas, Brazil. *Miner Deposita* 30:30–38